Talanta 122 (2014) 1–7

Contents lists available at ScienceDirect

Talanta

journal homepage: www.elsevier.com/locate/talanta

Second-order multivariate models for the processing of standard-addition synchronous fluorescence–pH data. Application to the analysis of salicylic acid and its major metabolite in human urine

Ariana P. Pagani, Gabriela A. Ibañez*

Departamento de Química Analítica, Facultad de Ciencias Bioquímicas y Farmacéuticas, Universidad Nacional de Rosario, and Instituto de Química Rosario (IQUIR), Consejo Nacional de Investigaciones Científicas y Técnicas (CONICET), Suipacha 531, Rosario S2002LRK, Argentina

ARTICLE INFO

Article history:
Received 11 November 2013
Received in revised form
30 December 2013
Accepted 4 January 2014
Available online 15 January 2014

Keywords:
Second-order multivariate analysis
Synchronous fluorescence–pH data
Standard addition
Salicyluric acid
Salicylic acid

ABSTRACT

In the present work, we describe the determination of salicylic acid and its major metabolite, salicyluric acid, in spiked human urine samples, using synchronous fluorescence spectra measured in a flow-injection system with a double pH gradient. Because the fluorescent urine background constitutes a potentially interfering signal, it becomes necessary to achieve the second-order advantage. Moreover, due to significant changes in the signal of the analytes in the presence of the urine matrix, mainly for salicyluric acid, standard addition was required in order to obtain appropriate quantifications. Several second-order multivariate calibration models were evaluated for this purpose: PARAFAC and MCR-ALS in two different modes, and PLS/RBL.

1. Introduction

Second- and third-order multivariate analysis has been gaining great importance in analytical applications, as can be seen from the literature in relevant analytical, chemometrics and applied journals. The combination of second-order data and multivariate algorithms allowed the development of the methods for analyte monitoring in complex biological, environmental and industrial samples [1]. This is also due to the variety of second-order instrumental data that are being employed, such as fluorescence excitation–emission spectroscopy, pH or kinetically modulated spectral information, or data from hyphenated techniques such as chromatography–mass spectrometry [1]. Furthermore, novel second-order signals based on the time evolution of chemiluminescence emission [2] and lanthanide-sensitized luminescence excitation [3] have been recently applied to determine a number of fluoroquinolones. It is important to emphasize the special properties exhibited by second-order data with respect to the presence of potential interferents. An adequate selection of data and algorithms may allow the quantification of analytes, even in the presence of unexpected sample constituents, a property known as the second-order advantage [1,4–6]. The presence of a complex matrix, which not only provides a significant interfering signal but also affects the analyte response in the sample (e.g., through inner filter effects or interactions between the analyte and the matrix, such as formation of complexes with proteins or associations), requires both second-order multivariate calibration and standard addition for successful analyte quantification, achieving the second-order advantage [7]. Instead of using standard addition, external calibration in the presence of the complex matrix could be employed [8]. However, this procedure is not always experimentally feasible.

Although several papers involving absorbance–pH data are reported in the literature [9–12], the analysis of fluorescence–pH data is not widespread. As has been discussed in the determination of fluoroquinolone in urine, second-order pH-fluorescence data can be used to quantify analytes when the fluorescence is highly pH-dependent [13]. Based on the strong pH-dependence shown by salicylic acid (SA) and its major metabolites, salicyluric (SU) and gentysic (GE) acids [14], Estevez da Silva et al. have proposed their determination in ternary mixtures using synchronous fluorescence–pH data. In this work, the changes in the pH values were obtained by acid–base titrations, using a peristaltic pump to force the solution into a flow cell, and data were analyzed using PARAFAC [15].

In the present work, we propose the determination of SA and SU in spiked human urine samples, using synchronous fluorescence spectra measured in a flow-injection system with a double pH gradient. The synchronous fluorescence mode is of particular

* Corresponding author.
E-mail address: ibanez@iquir-conicet.gov.ar (G.A. Ibañez).

0039-9140/$ - see front matter © 2014 Elsevier B.V. All rights reserved.
http://dx.doi.org/10.1016/j.talanta.2014.01.004

interest for the analysis of complex samples because higher spectral resolution is achieved in the simultaneous determination of multiple analytes [14,16,17]. In order to generate a controlled and reproducible pH gradient, a flow-injection method was used, providing a large amount of data in a very simple and fast way. As previously employed by Borraccetti et al. [13], a fast scanning spectrofluorimeter in the synchronous fluorescence mode was used, producing fluorescence–pH gradient data with improved selectivity and sensitivity, retaining the important second-order advantage.

Even though several algorithms are available for the convenient processing of second-order data, achieving the second-order advantage [7,18], it is important whether the three dimensional array built with these data for a set of samples complies or not with the so-called trilinearity condition [19]. In general, when the three-way array of second-order data is trilinear, trilinear decomposition algorithms can be conveniently applied, such as parallel factor analysis (PARAFAC) [20]. However, when the three-way data array deviates from the trilinearity condition, non-trilinear algorithms may be applied, such as multivariate curve resolution (MCR-ALS) when bilinearity of individual matrices is preserved [21], and latent variable algorithms such as unfolded partial least-squares (U-PLS) [22] and multiway PLS (N-PLS) [23], both combined with residual bilinearization (RBL) [8,24–27]. The selection of a suitable algorithm depends on the specific data properties.

When one of the data modes is a pH gradient, as in the present report, two challenges may appear for second-order multivariate calibration algorithms: (1) linear dependency, because closure relations may exist between pH-equilibrating species of each sample constituent, and (2) lack of reproducibility in the pH gradients from sample to sample. Solving these problems may demand MCR-ALS (which takes into account the lack of reproducibility of pH profiles and linear dependency). Alternatively, suitably initialized and restricted PARAFAC or PLS/RBL may be adequate, if the lack of reproducibility is small.

In this work, data analysis was performed using several second-order calibration methods in the standard addition mode, with the purpose of correcting both a responsive background and analyte–background interactions. It should be noticed that linear dependence is present in standard addition data when more than one interferent occurs in the test sample, in addition to the linear dependence produced by the pH gradient. Second-order standard addition data can be analyzed in the classical mode (mode 1), as well as in the modified approach, in which matrix data from the test sample are subtracted from the standard addition matrices (mode 2), and quantitation is subsequently done using the external calibration methodology [28].

In summary, in the present study SA and SU were quantified in urine samples employing synchronous fluorescence–pH data in the standard addition mode. The algorithms applied were PARAFAC and MCR-ALS in both modes, and PLS/RBL necessarily only in mode 2. The performance of the different algorithms was compared, suggesting that PARAFAC and MCR-ALS in mode 1 retrieved satisfactory predictions for SA, while in the case of SU, suitable predicted concentration values were achieved using PARAFAC in mode 1, MCR in mode 2 and PLS algorithms.

2. Experimental

2.1. Apparatus

A Gilson Minipuls Evolution peristaltic pump (Gilson, Middleton, WI, USA) was used for the propulsion of the carrier solution, at a flow rate of 0.5 mL min^{-1}. All sample solutions were manually injected into the carrier system using a dual proportional Upchurch injection valve (Upchurch scientific, Oak Harbor, WA, USA). The flow was injected into a quartz Hellma flow cell model 176.752-QS, 25 μL inner volume, 1.5 mm optical path length (Hellma, Müllheim, Germany). Synchronous fluorescence measurements were done using a fast scanning Varian Cary Eclipse spectrofluorometer (Varian Inc., Mulgrave, Victoria, Australia), equipped with two Czerny-Turner monochromators and a xenon flash lamp, and connected to a PC microcomputer via an IEEE 488 (GBIP) Serial Interface. Fluorescence scanning parameters were scanning speed, 3600 nm min^{-1}; slit widths, 5 nm; detecting voltage, 830. Spectral parameters are detailed in Section 2.3.

2.2. Reagents

All experiments were performed with analytical grade chemicals. The following solutions were employed: HCl 10^{-3} M, prepared from commercial HCl (Merck, Darmstadt, Germany); NaOH 10^{-3} M, prepared from commercial NaOH (Merck, Darmstadt, Germany). Stock solutions of sodium salicylate (Merck, Darmstadt, Germany) and salicyluric acid (Sigma, St. Louis, MO, USA), both 200 mg L^{-1}, were prepared weighing the required amount of the corresponding compounds and dissolving them in MilliQ water.

2.3. Flow injection methodology

In order to generate the double pH gradient inside the flow stream, the alkaline sample was injected into the acid sample used as the carrier. Each of the studied samples was diluted with HCl 10^{-3} M and used as the carrier steam. The composition of the injected sample was identical to that of the carrier, except that the dilution was carried out with NaOH 10^{-3} M. It was verified that this mode of generating the pH gradient presents the highest sensitivity, and therefore selected for this study. The flow injection analysis (FIA) assembly used is composed of a peristaltic pump, which drives the acid sample used as carrier through a Teflon tube (0.8 nm inner diameter). After the alkaline sample (500 μL) is injected, the flow is sent to the spectrofluorometer cell flow through a Teflon tube (total length = 4 m). The spectral measurements were done 2 min after the sample injection. Synchronous fluorescence spectra were collected under the following conditions: $\Delta\lambda$ (constant difference between excitation and emission monochromators), 100 nm; emission wavelength range, 260–360 nm each 3 nm; time between successive spectra, 0.05 min; total time, 2.5 min. The spectra were arranged into a matrix of size 31×50 data points, saved in ASCII format and transferred to a PC for subsequent manipulation with the multivariate programs.

2.4. Urine samples

Urine samples were spiked at a concentration given by random numbers in the range 0–300 mg L^{-1} for both analytes (in order to test the method performance for many concentrations within the therapeutic range). The spiked samples were diluted 1:200 with HCl 10^{-3} M to be employed as carriers, or with NaOH 10^{-3} M to be injected into the flow system. Afterwards, new solutions were prepared starting from the spiked samples in order to carry out three successive additions of each analyte. Concentrations were increased by 0.50, 1.00 and 1.50 mg L^{-1} for both salicyluric and salicylic acids, on different aliquots of the original samples (values refer to the measuring cells). Each of these samples was also diluted with HCl 10^{-3} M or with NaOH 10^{-3} M as described above. We estimate the uncertainties in all these analyte concentrations to be of the order of ± 0.01 mg L^{-1}. All the concentration ranges are within the therapeutic values of the studied drugs in human urine.

2.5. Algorithms

The theory of the second-order multivariate calibration algorithms applied in the present work is now well established and can be found in the relevant references: PARAFAC, Ref. [20]; MCR-ALS, Ref. [21]; U-PLS, Ref. [22]; N-PLS, Ref. [23] and PLS/RBL, Ref. [8,24,25].

2.6. Software

The routines employed for second-order multivariate calibration are all available on the Internet: PARAFAC and N-PLS at http://www.models.life.ku.dk/source/, MCR-ALS at http://www.ub.es/gesq/mcr/mcr.htm and N-PLS/RBL including the graphical interface of the MVC2 toolbox which implements both PARAFAC and N-PLS/RBL at http://www.chemometry.com/Index/Links%20and%20downloads/Programs.html. All of them are written in MATLAB7.0.

3. Results and discussion

Fig. 1 shows the excitation–emission fluorescence contour plots corresponding to a typical urine sample and to aqueous solutions of SA and SU at pH=10. As can be observed, the spectra overlapping between the urine and the investigated compounds are significant. Synchronous fluorescence spectroscopy is a good alternative, which presents higher selectivity towards overlapped component spectra. The constant difference between the excitation and emission monochromators ($\Delta\lambda$) used was 100 nm, in agreement with that reported in the literature [29], consequently the synchronous path passes through the maximum of the fluorescence band for the analytes. Fig. 2A presents the experimental synchronous spectra using the $\Delta\lambda$=100 nm, corresponding to the urine and the analytes.

As previously mentioned, the SA and SU fluorescence is known to be strongly pH-dependent, which opens the possibility of obtaining second-order data based on synchronous fluorescence spectra modulated by a double pH gradient, generated within a flow injection system. According to the literature [14], in the case of SA, fluorescence intensity is low at pH below its pK_a (pK_{a1}=2.9),

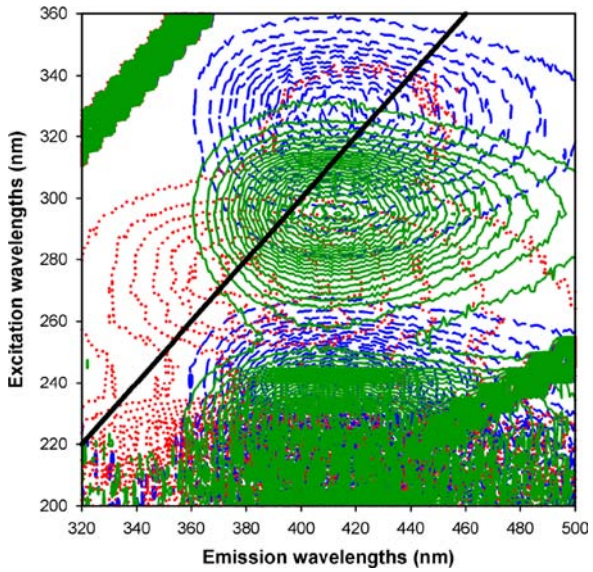

Fig. 1. Urine sample dilute 1:200 (dotted line, red); SA 3.00 mg L^{-1} (solid line, green); SU 2.00 mg L^{-1} (dashed line, blue). Experimental conditions: pH=10–11; PMT=830. (For interpretation of the references to color in this figure caption, the reader is referred to the web version of this paper.)

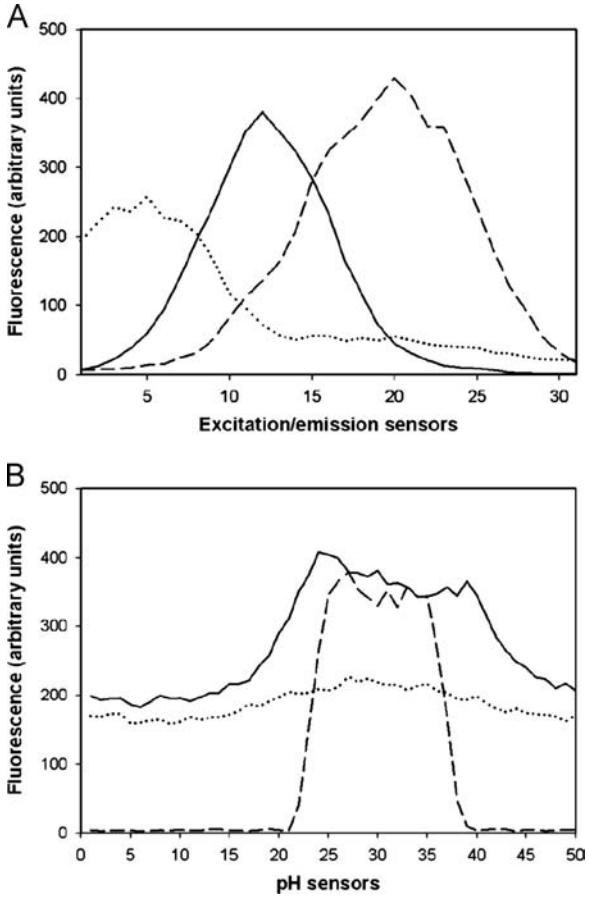

Fig. 2. (A) Synchronous fluorescence spectra in basic medium and (B) pH profiles obtained at the corresponding maximum of synchronous spectra, using $\Delta\lambda$= 100 nm; SA 1.00 mg L^{-1} (solid line); SU 1.00 mg L^{-1} (dashed line) and urine diluted 1:200 (dotted line).

and increases and remains constant at pH above its pK_a value. The SU fluorescence has zero intensity before pH 7, increasing as the pH increases, and achieving a maximum and constant value at pH greater than 9 (pK_a=8.2). In these cases, the change in the protonation degree causes only changes in fluorescence intensity, without generating any maximum shifts. Given the pK_a values of the analytes, sodium hydroxide and hydrochloric acid solutions were used in order to achieve a proper pH gradient, as mentioned above. Fig. 2B shows the experimental pH profiles obtained with the experimental condition previously described. It is important to emphasize that in the pH dimension, the urine signal does not significantly change, and that the analytes' profiles observed are consistent with their pH-dependence.

As formerly stated, the presence of a responsive background requires the use of the standard addition method. Second-order data in the standard addition mode allows to correct the background effect, both due to the changes in analyte response brought about by interactions with the background and due to the presence of responsive components that give interfering signals. In the presently studied case, the urine interferes because (a) it shows a major signal overlapped with the analytes and (b) it affects pH profiles, mainly that corresponding to SU. It is noteworthy that additions for each analyte were performed separately on identical aliquots of the sample. Thus, in each experiment, only one of the analyte concentrations is changed, remaining constant both the signal corresponding to the other analyte and the urine signal as well. This procedure minimizes the number of additions, and avoids the need of a complex experimental design.

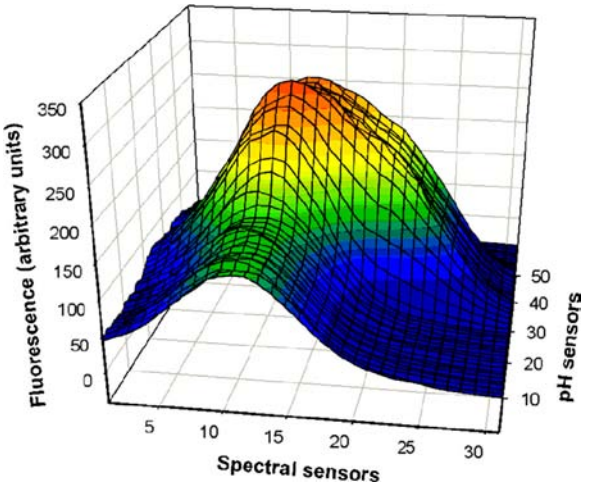

Fig. 3. Three-dimensional plot of synchronous fluorescence spectra–pH gradient for a typical validation urine sample (diluted 1:200) containing SA 0.80 mg L^{-1} and SU 0.80 mg L^{-1}. Experimental conditions: $\Delta\lambda = 100$ nm; PMT = 830; silt widths = 5 nm.

Fig. 3 shows a typical landscape of synchronous fluorescence spectra–pH data for a urine sample spiked with both salicyluric and salicylic acid. This is the type of signal which can be conveniently processed by second-order multivariate algorithms, providing the required second-order advantage.

3.1. PARAFAC analysis

When PARAFAC analysis of the different experimental data sets was attempted, the first step was the estimation of the number of responsive components. This can in principle be assessed using either the diagnostic tool known as the core consistency test or the consideration of the residual fit of the PARAFAC model, as the number of components is increased. When the PARAFAC standard addition mode 1 was employed in the SA analysis, the core consistency values were 100, 99.9, 32.3, 0.18 and 23.5 for 1–5 components, respectively, while the residuals fit decreased as follows: 32.8, 11.8, 3.9, 3.4 and 3.2 arbitrary fluorescence units. The progression of core consistency values suggests two components. However, the changes in fitting residuals indicate stabilization at three components, which is more reasonable (SA as analyte, plus SU and urine). In the SU analysis, the core consistency values were 100, 99.4, 13.1, (negative value) and 4.6 for 1–5 components, respectively, while the residuals of the PARAFAC fit in mode 1 decreased as follows: 42.8, 5.6, 4.0, 3.6 and 3.2 arbitrary fluorescence units. When analyzing residual fits, two or three components appear to be optimum. Nevertheless, when three components were extracted by PARAFAC, the third profile was similar to one of the first two. In conclusion, two components were enough to explain the variability of the three-way data for SU and to obtain successful predictions, in agreement with the core consistency test.

When applying PARAFAC in mode 1 for SA analysis with no restrictions imposed, and starting the least-squared fit from the scores and profiles given by DTLD, the final profiles were not physically reasonable, i.e., some of the values were negative. Despite the fact that in some test samples the analyte profiles and scores were correctly retrieved and the analyte quantitation was accurate, in other samples considerably inaccurate results were obtained, even after applying non-negativity restrictions. The results yielding predictions which were significantly different from the nominal values corresponded to PARAFAC solutions which were linear combinations of the known component profiles. Hence, the results for SA were satisfactory for the complete set of validation samples when PARAFAC was initialized with the best fit of several small runs employing random loadings, and applying non-negativity restrictions during the least-squares fit. In the case of SU quantitation, the application of DTLD initialization, even without non-negativity constraint, was enough to yield successful prediction results, as shown in Table 1.

Fig. 4 shows the profiles retrieved by PARAFAC when processing a typical standard addition data for SA in mode 1. As can be seen, the spectral profiles are correctly retrieved, if Fig. 4A is compared with the experimentally available isolated profiles shown in Fig. 2A. The pH profiles shown in Fig. 4B are highly reasonable, showing the expected changes due to the transformation of the analyte protonated species into the anionic ones, upon injection of the alkaline sample solution. A typical run for SU provided the profiles shown in Fig. 5. SU profiles are correctly retrieved (see Fig. 2), while SA and urine profiles are recovered as a single component, representing a unique interferent. The difference in the number of components required for SA and SU analysis suggests that the linear dependence phenomenon is present only for SA, and would also support the distinct initializations used in both cases.

Once the analyte profiles were identified, prediction proceeded by the usual interpolation into the pseudo-univariate calibration graph, built in this case with scores for the species of the analyte which provided better sensitivity. The prediction results for the set of spiked test samples are shown in Table 1, leading to the following root mean square error values: 0.10 and 0.07 for SA and SU, respectively. These results for both analytes are consistent with the complexity of the system, considering the effect of the responsive urine background. The latter affects mainly SA, which presents more interference in both spectral and pH dimensions. In the case of SU, unlike SA, the interfering urine signal is less significant in the spectral dimension, and the pH profiles exhibit greater differentiation. Close inspection of the PARAFAC results (see Figs. 4 and 5) explains the difficulties in the resolution of SA from the background signal, because although three responsive components were estimated in the case of SA, only two components were required in the corresponding SU addition.

The application of PARAFAC in the modified standard addition mode 2 was unable to improve the results achieved with the

Table 1
Predicted concentrations for SA and SU in the test urine samples using PARAFAC model in mode 1.

Sample	SA		SU	
	Nominal	Predicted[a]	Nominal	Predicted[a]
1	0	−0.005	1.50	1.48
2	0.70	0.62	1.30	1.26
3	0.35	0.21	0.60	0.73
4	0.80	0.66	0.80	0.78
5	1.50	1.57	0	0.02
6	0.60	0.54	0.35	0.36
7	0.25	0.21	0.25	0.25
8	0.50	0.46	0.50	0.55
9	1.00	1.20	0	0.02
10	0	0.005	1.00	1.11
11	0.50	0.47	1.00	1.10
12	0	0.011	0.50	0.55
13	0.50	0.59	0	0.05
14	1.20	1.43	0.20	0.28
RMSE[b]		**0.10**		**0.07**
REP%[c]		10		7

[a] Concentrations are all given in the measuring cell, expressed in mg L^{-1}.
[b] RMSE, root mean square error, expressed in mg L^{-1}.
[c] REP%, relative error of prediction, expressed (in %) with respect to the mean added concentrations (1.0 mg L^{-1}).

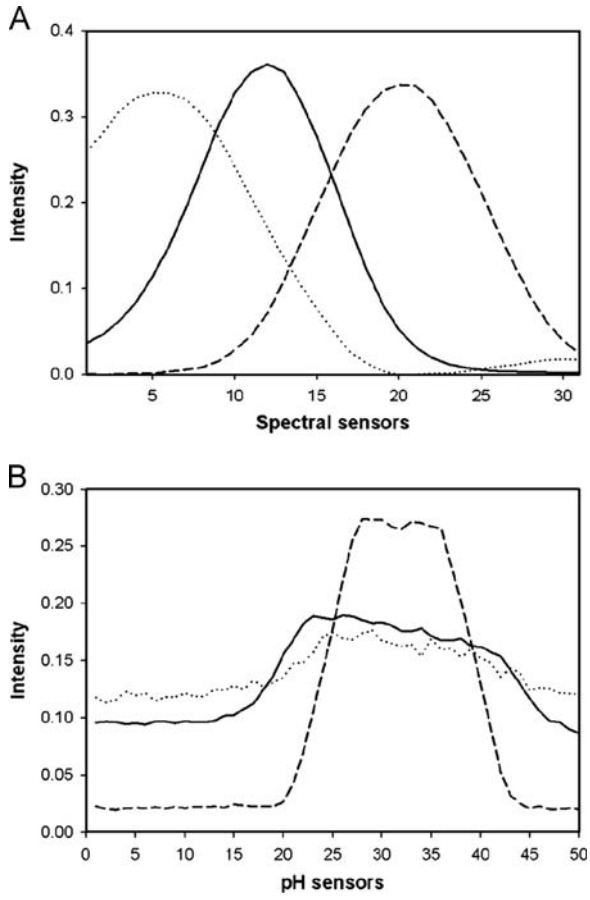

Fig. 4. Profiles retrieved for the three responsive components of a urine sample diluted 1:200 spiked with SA 0.50 mg L^{-1} and SU 1.00 mg L^{-1} when PARAFAC in mode 1 was applied for SA determination. Profiles can be identified as SA (solid line), SU (dashed line) and urine (dotted line) for (A) Fluorescence dimension and (B) pH dimension. All profiles were normalized to unit length.

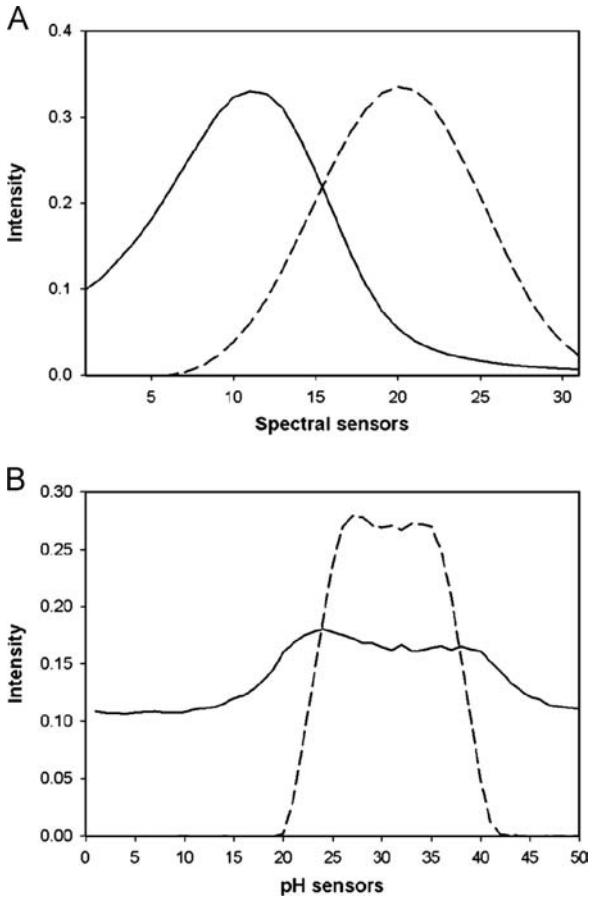

Fig. 5. Profiles retrieved for the two responsive components of a urine sample diluted 1:200 spiked with SA 0.70 mg L^{-1} and SU 1.30 mg L^{-1} when PARAFAC in mode 1 was applied for SU determination. Profiles can be identified as SU (dashed line) and a combination of SA and urine (solid line) for (A) Fluorescence dimension and (B) pH dimension. All profiles were normalized to unit length.

former alternative, especially for the SA, where poorer predictions were obtained (not shown).

3.2. MCR-ALS analysis

In the case of MCR-ALS, matrix augmentation was performed in the pH direction. This was done in order to compensate the variations in the measured pH profiles from sample to sample, since MCR-ALS allows each sample to present its own specific profile in the augmented direction, and also enables to solve the linear dependency in pH profiles. Furthermore, the pH mode shows low selectivity, mainly between SA and urine, and augmentation is known to improve the selectivity along the augmented direction. Analysis of the test samples was first performed using the classical standard addition mode 1. The augmented matrices were analyzed using MCR-ALS with appropriate initializations: non-negativity in both concentration and spectral profiles, and employing as estimated initial profiles those corresponding to standard solutions and random urine free of analytes. Initialization made by resorting to the so-called purest variables found by SIMPLISMA (simple interactive self-modelling mixture analysis) led to unsuccessful results for SA. For both SA and SU, three responsive components were included in the study, as established by principal component analysis of the augmented data matrices, in contrast to PARAFAC, in which only two components were considered for SU. After the fitting has converged, MCR-ALS retrieved satisfactory spectral profiles. Fig. 6A displays an example of a typical SA sample, showing the fitted spectra for sample components, which can be compared to those in Fig. 2A. The retrieved pH profiles for the successive data matrices are shown in Fig. 6B, illustrating how the analyte concentrations (solid line) increase, going from the test sample (the left sub-matrix) to the standard additions (the three adjacent sub-matrices), whereas the interferents (SU and urine) remain almost constant, as expected. The achieved predictions employing this augmentation mode are shown in Table 2; the RMSE are 0.07 and 0.17 mg L^{-1} for SA and SU, respectively. As can be seen, good results are obtained in the case of SA, which are seen to be comparable to those for PARAFAC. However, MCR-ALS results for SU are poorer than those obtained with PARAFAC. The root mean square errors reported for PARAFAC and MCR-ALS can be compared using the randomization approach described in Ref. [30]. Specifically, for SA, the estimated significance level associated with the test that the RMSE for PARAFAC was larger than the RMSE for MCR-ALS is >0.05, and therefore not significant (calculated using 1999 iterations, for details see Ref. [30]). This indicates that the decrease in RMSE in going from PARAFAC to MCR-ALS for SA is not statistically meaningful. Nevertheless, for SU the estimated significance level associated with the test that the RMSE for PARAFAC was lower than the RMSE for MCR-ALS is <0.01, and therefore significant. This statistical analysis allows concluding that the best predictions for SU are obtained with PARAFAC.

With the aim of improving the obtained results, mainly for SU, MCR-ALS was also implemented in mode 2. As discussed in previous works, MCR-ALS in mode 2 can provide better results than mode 1 in systems which display different challenges [3,28].

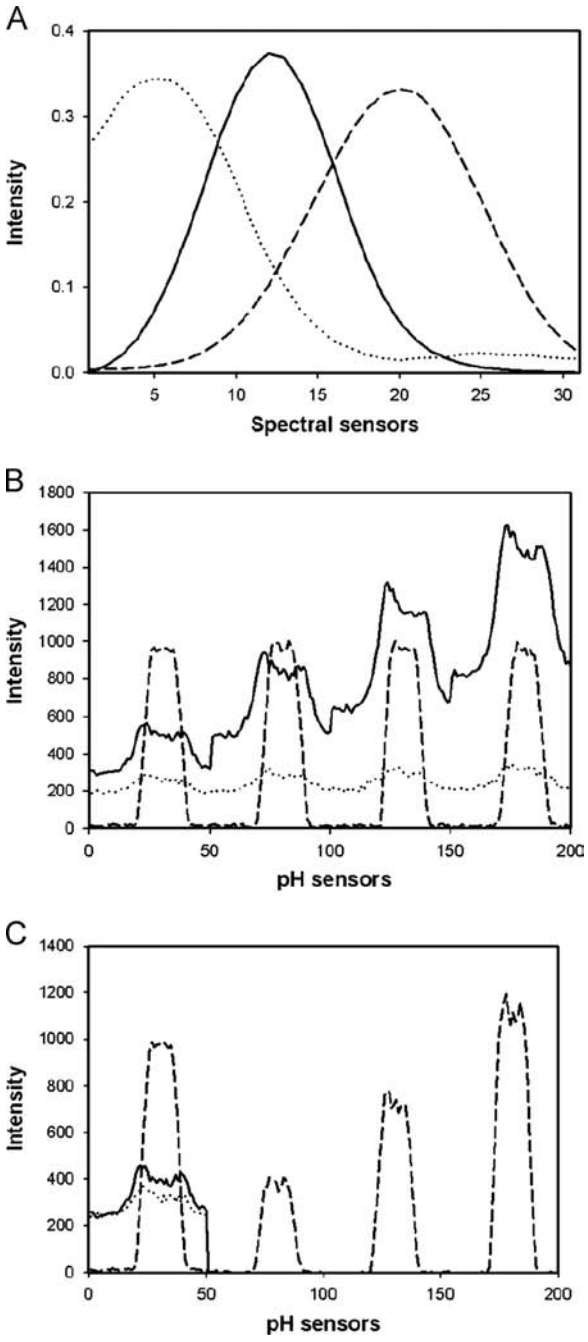

Fig. 6. Profiles retrieved by MCR-ALS when processing a typical urine sample, spiked with the analytes SA and SU. (A) Spectral profiles, common to all samples in the regular standard addition mode 1 (those for the modified standard addition mode 2 are identical). (B) pH profiles for successive matrix samples in the regular standard addition mode 1: from left to right, test sample and the three standard additions of SA. (C) pH profiles for successive matrix samples in the regular standard addition mode 2: from left to right, test sample and the results of subtracting the test sample data from the three standard additions of SU. In all cases, SA (solid line), SU (dashed line) and urine (dotted line).

MCR-ALS analysis in mode 2 was performed employing similar initialization conditions and restrictions during the least-squares fit than those used in mode 1, with the additional information provided by the so-called correspondence among species and samples (which informs the algorithms that certain components are absent in some samples). The spectral profiles recovered by the algorithm (not shown) were again very similar to those shown in Fig. 6A, while those corresponding to the pH dimension, presented in Fig. 6C, are interpreted as involving an interferent profile which

Table 2
Predicted concentrations for SA and SU in the test urine samples using MCR-ALS model in both standard addition modes.

Sample	SA			SU		
	Nominal	Predicted[a]		Nominal	Predicted[a]	
		Mode 1	Mode 2		Mode 1	Mode 2
1	0	0.09	0.13	1.50	1.55	1.44
2	0.70	0.84	1.02	1.30	1.49	1.40
3	0.35	0.41	0.54	0.60	0.80	0.73
4	0.80	0.86	1.03	0.80	0.85	0.94
5	1.50	1.40	2.24	0	0.11	0.03
6	0.60	0.69	0.79	0.35	0.46	0.36
7	0.25	0.29	0.47	0.25	0.41	0.35
8	0.50	0.49	0.82	0.50	0.69	0.54
9	1.00	0.98	1.15	0	0.20	0.02
10	0	0.09	0.11	1.00	1.18	1.01
11	0.50	0.61	0.79	1.00	1.37	1.38
12	0	0.05	0.001	0.50	0.61	0.53
13	0.50	0.44	0.50	0	0.12	−0.04
14	1.20	1.42	1.48	0.20	0.37	0.19
RMSE[b]		**0.07**	**0.28**		**0.17**	**0.12**
REP%[c]		**7**	**28**		**17**	**12**

[a] Concentrations are all given in the measuring cell, expressed in mg L^{-1}.
[b] RMSEP, root mean square error.
[c] REP%, relative error of prediction, expressed (in %) with respect to the mean added concentrations (1.0 mg L^{-1}).

only contributes to the test sample, and analyte profiles in the three right sub-matrices (SU) which allow to calibrate a pseudo-univariate model. This implies that quantitation can be done using the classical external calibration. As shown in Table 2, MCR-ALS in mode 2 leads to considerably poorer results for SA, while SU prediction results seem slightly better. Despite what was expected, when comparing RMSE values using the statistical test previously mentioned, the results validate a poor performance for SA in this mode 2, compared with both PARAFAC and MCR-ALS mode 1. This can be confirmed by visual inspection of Fig. 7A, which shows a box and whisker plot summarizing the complete results for all the applied algorithms. The results discussed above could be explained taking into account that in mode 1 a better discrimination between urine and SA profiles is achieved as the signal of SA increases, while the urine background remains constant. On the other hand, the RMSE in mode 2 for SU is statistically comparable with those obtained in PARAFAC analysis, confirming that the predictions improve using MCR-ALS in the modified mode, as expected. Although the difference of RMSE values for MCR-ALS in both modes is not statistically meaningful, the inspection of Fig. 7B reveals a bias in the complete results using mode 1, with an improvement on employment of mode 2. The origin of the bias in the former case is unclear, but may be related to the strong correlations when mode 1 is used, since in the spectral dimension urine exhibits a low signal completely overlapped with SU spectra (see Fig. 2A).

3.3. N-PLS/RBL and U-PLS/RBL analyses

Finally, the latent variable structured models U-PLS/RBL and N-PLS/RBL were applied, using the only possible standard addition strategy, mode 2. Calibration was performed using a single latent variable, with mean-centering for SA, while one and two components were included in the RBL phase for SU and SA, respectively. In the case of SU, the use of both multidimensional and unfolded PLS/RBL, achieving the second-order advantage, provided results of a quality comparable to PARAFAC and MCR-ALS in mode 2 alternatives (Fig. 7B). The RMSE values are 0.09 and 0.10 mg L^{-1} for N-PLS/RBL and U-PLS/RBL, respectively, which are not

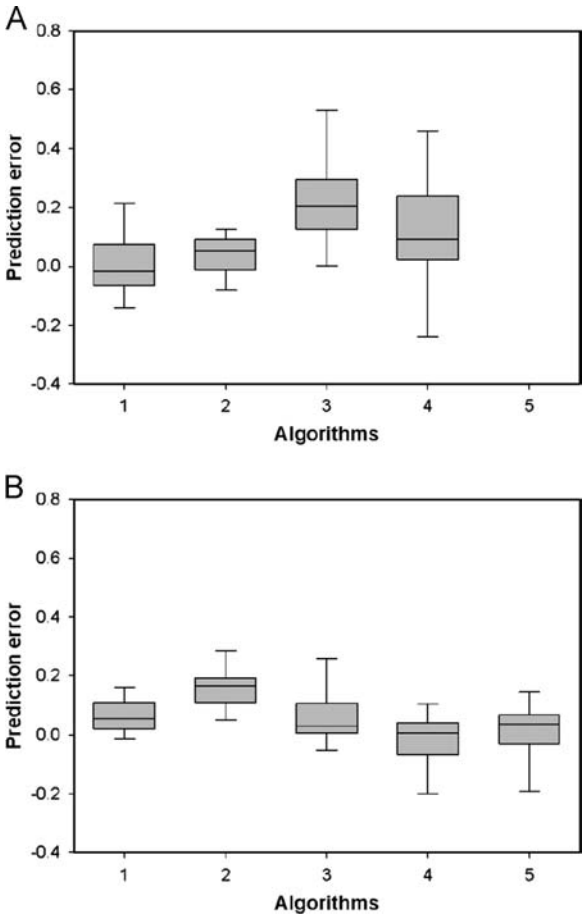

Fig. 7. Box and whisker plot of prediction results corresponding to the validation urine samples for (A) SA and (B) SU. Algorithms are numbered in the horizontal axis as follows: (1) PARAFAC mode 1, initialized with the best of 10 small runs or DLTD for SA and SU, respectively, (2) MCR-ALS in mode 1, (3) MCR-ALS in mode 2, (4) U-PLS/RBL in mode 2 and (5) N-PLS/RBL in mode 2. For each algorithm, the grey boxes are bounded by the 25% and 75% quartiles with the median inside, whereas the extreme levels correspond to 5% and 95% quartiles.

statistically different in comparison with the former alternatives. It should be noticed that when RBL procedure was applied in order to obtain second-order advantage, unexpected component profiles were recovered as a combination of SA and urine profiles, as previously noted in PARAFAC. When applying U-PLS/RBL for SA, the results were rather discouraging, since for some of the studied samples significantly inaccurate predictions were obtained, as can observed in Fig. 7A. It is noteworthy that U-PLS/RBL results are comparable to those obtained with MCR-ALS mode 2, but the multidimensional counterpart N-PLS/RBL (not shown) gave even poorer results than the unfolded variant. This lower performance of the multidimensional variant of PLS in comparison with the unfolded PLS may be associated with the impossibility of RBL procedure to retrieve the interferent profiles, mainly of urine, hence spoiling the second-order advantage.

4. Conclusions

Second-order multivariate calibration algorithms were used to quantify salicylic acid and one of its major metabolites, salicyluric acid, in spiked human urine samples, using synchronous fluorescence spectra measured in a flow-injection system with double pH gradient. Due to significant changes in the signal of the analytes in the presence of a complex matrix, the use of the standard addition method was required in order to obtain appropriate quantifications.

The results indicate that the overlapping between SA and urine in both dimensions enables only PARAFAC and MCR-ALS mode 1 to give satisfactory results, since the RBL process needed to achieve the second-order advantage in the algorithms based on the latent variables (PLS) is not capable to properly separate the urine contribution. MCR-ALS requires to be initialized with pure profiles of the analytes and urine in order to decrease the ambiguity and provide accurate outcomes.

Otherwise, SU can be quantified using the different algorithms available, but it is noteworthy that with PARAFAC mode 1 and PLS/RBL, urine and SA are modeled as a single component, which is possible due to the experimental design employed for the addition. On the other hand, during the analysis using MCR-ALS mode 2, suitable results are obtained for this analyte with a proper discrimination between SA and urine, even using SIMPLISIMA as the initial estimates.

Acknowledgments

The authors gratefully acknowledge the Universidad Nacional de Rosario and the Consejo Nacional de Investigaciones Científicas (PIP N° 1950) and Técnicas and Agencia Nacional de Promoción Científica y Tecnológica (PICT N° 2010-0084) for financially supporting this work. The authors are also thankful to Dr. A. C. Olivieri for his valuable suggestions.

References

[1] G. Escandar, N. (Klaas) M. Faber, H.C. Goicoechea, A. Muñoz de la Peña, A.C. Olivieri, R.J. Poppi, Trends Anal. Chem. 26 (2007) 752–765.
[2] V.A. Lozano, G.A. Ibañez, A.C. Olivieri, Anal. Chem. 82 (2010) 4510–4519.
[3] V.A. Lozano, R. Tauler, G.A. Ibañez, A.C. Olivieri, Talanta 77 (2009) 1715–1723.
[4] R. Bro, Crit. Rev. Anal. Chem. 36 (2006) 279–293.
[5] Å. Rinnan, J. Riu, R. Bro, J. Chemom. 21 (2007) 76–86.
[6] K.S. Booksh, B.R. Kowalski, Anal. Chem. 66 (1994) 782A–791A.
[7] A.C. Olivieri, Anal. Chem. 80 (2008) 5713–5720.
[8] M.J. Culzoni, H.C. Goicoechea, A.P. Pagani, M.A. Cabezón, A.C. Olivieri, Analyst 131 (2006) 718–723.
[9] N.R. Marsili, A. Lista, B.S. Fernandez Band, H.C. Goicoechea, A.C. Olivieri, J. Agric. Food Chem. 52 (2004) 2479–2484.
[10] V. Gómez, R. Cuadros, I. Ruisánchez, M.P. Callao, Anal. Chim. Acta 600 (2007) 233–239.
[11] J. Saurina, S. Hernández-Cassou, A. Izquierdo-Ridorsa, R. Tauler, Chemom. Intell. Lab. Syst. 50 (2000) 263–271.
[12] J. Saurina, S. Hernández-Cassou, Anal. Chim. Acta 438 (2001) 335–352.
[13] M.D. Borraccetti, P.C. Damaini, A.C. Olivieri, Analyst 134 (2009) 1682–1691.
[14] F. Salinas, A. Muñoz de la Peña, I. Duran-Meras, M.S. Duran, Analyst 115 (1990) 1007–1011.
[15] J. Esteves da Silva, S.G. Novais, Analyst 123 (1998) 2067–2070.
[16] J.B.F. Lloyd, Analyst 105 (1980) 97–109.
[17] E.L. Inman, J.K. Winefordner, Anal. Chem. 54 (1982) 2018–2023.
[18] N. Marsili, A. Lista, B. Fernandez Band, H. Goicoechea, A.C. Olivieri, Analyst 130 (2005) 1291–1298.
[19] A.C. Olivieri, G.M. Escandar, A. Muñoz de la Peña, Trends Anal. Chem. 30 (2011) 607–617.
[20] R. Bro, Chemom. Intell. Lab. Syst. 38 (1997) 149–171.
[21] R. Tauler, Chemom. Intell. Lab. Syst. 30 (1995) 133–146.
[22] S. Wold, P. Geladi, K. Esbensen, J. Øhman, J. Chemom. 1 (1987) 41–56.
[23] R. Bro, J. Chemom. 10 (1996) 47–61.
[24] J. Öhman, P. Geladi, S. Wold, J. Chemom. 4 (1990) 79–90.
[25] A.C. Olivieri, J. Chemom. 19 (2005) 253–265.
[26] A. García-Reiriz, P.C. Damiani, M.J. Culzoni, H. Goicoechea, A.C. Olivieri, Chemom. Intell. Lab. Syst. 92 (2008) 61–70.
[27] A. García-Reiriz, P.C. Damiani, A.C. Olivieri, Chemom. Intell. Lab. Syst. 100 (2010) 127–135.
[28] V.A. Lozano, G.A. Ibañez, A.C. Olivieri, Anal. Chim. Acta 651 (2009) 165–172.
[29] P. Damiani, M.E. Ribone, G.A. Ibañez, A.C. Olivieri, Analyst 120 (1995) 443–445.
[30] H. van der Voet, Chemom. Intell. Lab. Syst. 25 (1994) 313–323.